THEORY OF COMBINED SWAY AND NONSWAY FRAMES BUCKLING

By P. Lokkas[1] and J. G. A. Croll[2]

ABSTRACT: Conventional design procedures for rigid jointed frames encourage a situation in which more than one buckling mode could occur simultaneously. Even though this practice is known to often give rise to increased sensitivity of buckling loads to small initial imperfections, current design practice is usually lacking in explicit design guidance. This paper seeks to explore the extent to which buckling loads in framed structures are reduced by the effects of modal interactions arising when designs are optimized. It takes, as a specific example, the situation where the buckling and bending planes for a rigid-jointed frame coincide and for which sway and nonsway buckling modes occur at similar load levels. It explores the extent to which elastic-plastic buckling loads may be affected by interactions of sway and nonsway modes and compares predictions with results from a recently conducted test program. It is suggested that the theoretical approach described has the potential to provide an extended and improved alternative to existing design practice.

INTRODUCTION

Structural optimization can lead to situations in which more than one possible failure mode occurs at the same load level. Even where optimization is not consciously pursued this same situation can arise as a natural consequence of the conventional design process.

In a typical design process the various components making up the structure are designed to have roughly similar margins of safety against collapse. For an efficiently designed system it might be expected that at the factored load a multitude of components could simultaneously fail. Where an individual component has a number of possible failure modes, then if efficiently detailed, it would be expected that these too might occur simultaneously. Where failure is triggered by buckling this so-called naive approach to structural optimization can cause serious problems.

The following sets out to explore the extent to which buckling of frames exhibiting simultaneous sway and nonsway buckling modes might be affected by such interactions. After a brief discussion of the wider effects of optimization on buckling behavior and how current design practice copes, the paper concentrates upon rigid frame buckling. It takes as an exemplifying example the case of the interactions between sway and nonsway buckling modes that occur within the plane of primary bending. It develops for this two-mode problem a theoretical approach consistent with conventional single mode buckling and shows how this requires the specification of two imperfection parameters. Results from a test program upon a suitably designed limited frame are used to assess the validity of the theoretical approach to frame collapse.

INTERACTIVE BUCKLING AND STRUCTURAL OPTIMIZATION

The problems that can arise when structures admit possible interactions between buckling modes have long been recognized. Perhaps the first major disaster for which collapse was partially triggered by an interaction of buckling modes was that of the Quebec Bridge in 1907. Although the original design adopted an overall geometry very reminiscent of the Forth Rail Bridge, the tubular compression struts of the Forth Rail Bridge were replaced with components built up from laminated plates tied together at intervals along the length. A local buckling of the laminate plates between the ties led to a serious weakening of the strut in its overall "Euler" buckling mode. The results are well known [see, e.g., Hopkins (1990)].

The form of buckling exhibited by the laminated struts of the Quebec Bridge could be regarded as active interaction. Fig. 1(a) shows the two forms of potential buckling mode. As illustrated in Fig. 1(b), a situation where the elastic critical loads associated with the potential buckling modes are nearly simultaneous can result in interactive buckling which, even for the elastic system, exhibits a potentially violent loss of load-carrying capacity. This unstable buckling behavior has all the properties of shell buckling, with the least attractive element being the extreme sensitivity of buckling loads to the effects of even small imperfections.

Partly, as a result of the potentially disastrous consequences, design guidance for these active interactive buckling problems has taken a rather cautious form. For the design of latticed or battened struts, for example, the slenderness ratios associated with the local buckling (similar to that discussed for the laminated strut in Fig. 1) are restricted to ensure that it occurs at a load level at least twice that for the overall buckling. This is the practice adopted in BS 5950 ("Structural" 1990), Eurocode E3 ("Steel" 1992), and the earlier BS 449 ("Specification" 1969), all of which call for a local buckling twice that for the overall buckling. In a similar way, for the design of stiffened plates in compression most design guidance documents require stiffeners to be designed to ensure that local interstiffener or stiffener tripping buckling occurs at loads well

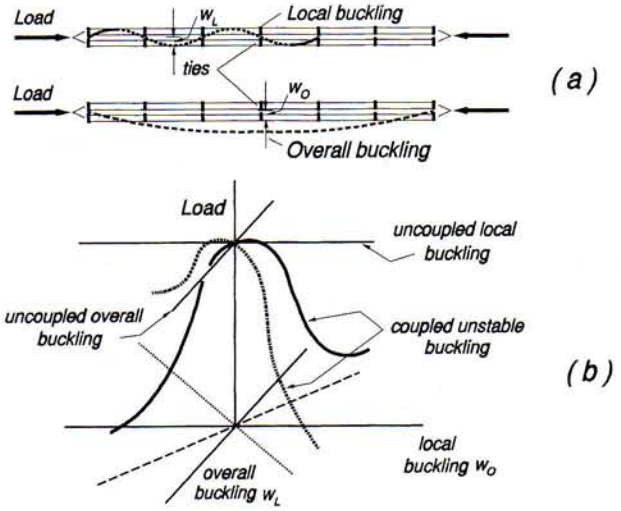

FIG. 1. Active Interactive Buckling for Built-Up Laminated Columns

[1]Prof., Dept. of Civ. Engrg. Public Works, Technol. Educational Instn., Larissa, Greece.

[2]Prof. and Head of Dept. of Civ. and Envir. Engrg., Univ. Coll. London, London WC1E 6BT, U.K.

Note. Associate Editor: Chai H. Yoo. Discussion open until June 1, 2000. To extend the closing date one month, a written request must be filed with the ASCE Manager of Journals. The manuscript for this paper was submitted for review and possible publication on July 27, 1998. This paper is part of the ***Journal of Engineering Mechanics***, Vol. 126, No. 1, January, 2000. ©ASCE, ISSN 0733-9399/00/0001-0084–0092/$8.00 + $.50 per page. Paper No. 18902.

above that for the overall orthotropic panel. This is achieved by again placing restrictions upon the slenderness ratios of the local stiffeners. In contrast, for the design of a stiffened cylindrical shell it is usual practice to detail stiffening to produce an overall buckling load that is considerably higher than that of local buckling. In each of these cases of potentially active interactive buckling, design practice seeks to prevent the designer from achieving a simultaneity of the various possible critical loads.

Because in the design of continuous rigid frames it is usual practice to detail individual components to have consistent factors of safety against buckling failures, our conventional design practice could be said to encourage the occurrence of simultaneous buckling. In the detailing of even a simple column, exhibiting the possibility of buckling about both the major and minor axes, it would be normal to attempt to choose the second moments of area in such a way that the two slenderness ratios are as near as possible equal. Too high a buckling resistance about the major axis means that failure will be precipitated about the minor axis. Clearly, in this situation, a redistribution of material over the cross section to increase the stiffness about the minor axis, and consequently decrease that about the major axis, will enable an increase in load carrying capacity. Similar reasoning would apply if buckling were to be precipitated about the major axis. It is easy to see that the maximum buckling capacity, using our conventional design practice of treating each mode separately, will be achieved when the major and minor axes buckling capacities are equalized. This form of optimization is discussed in Fig. 2.

In contrast with the strong elastic interactions exhibited when components such as the laminated strut of Fig. 1 are optimized, the biaxial buckling of columns could be said to be of a form of passive interaction. Indeed, most situations in rigid frames, in which local buckling of a slender cross section is prevented, will display passive interactions in their elastic buckling behavior. In frames constructed from standard hot-rolled steel sections the dangers of an active elastic interaction of the type described in Fig. 1 have been effectively eliminated by design, through the choice of cross section properties. However, if thin-walled or built-up sections are used, it is possible that local torsional buckling of the flanges could in an optimized section occur simultaneously with overall buckling. In these circumstances it is possible that a potentially dangerous elastic interaction of the type described in Fig. 1 could occur. In what follows it is assumed that local elastic buckling of the cross sections occurs at loads sufficiently high that interaction with the overall column buckling is of secondary importance. For this reason we are concentrating upon the passive forms of elastic buckling interaction as exemplified by the case of biaxial buckling described in Fig. 2. However, even a passive, or stable, elastic interactive buckling can generate the imperfection sensitivity associated with active interaction, when the effects of material failure are taken into account. Hence, although the present interest in frame buckling problems generally precludes unstable forms of elastic interaction, taking into account the development of material failure can lead to strong modal interactions and sensitivity of buckling loads to more than one imperfection. It is these more benign interactions that are considered in the following.

ELASTIC FRAME BUCKLING

Of present concern is the buckling of rigid-jointed rectilinear frames. In the primary bending plane a typical column could fail in a nonsway mode w_n or be part of a failure in a sway mode w_s. Of particular interest is the situation where the critical loads governing the loss of stability of the idealized, "perfect," column into the nonsway P_{cn} and sway P_{cs} occur at similar load levels. In these circumstances attention will be focused on the effects of imperfections in each of these modes, and how they combine to influence the elastic-plastic failure loads.

Elastic Critical Loads

Critical loads for the frame are often calculated on the basis of a limited frame, which in turn can be reduced to the buckling of an idealized column having elastic translational and rotational restraints at its ends, as shown in Fig. 3. These lumped spring stiffnesses can be calculated to represent the elastic stiffness offered by the rest of the frame to end displacements of the column. It is a relatively straightforward matter to calculate the spectrum of critical loads P_{ci} and their associated critical mode shapes $w_{ci}(x)$. This has been described by Gurfinkel and Robinson (1965), whereas a more complete treatment has recently been presented by Lokkas (1996). As an example, consider the frame shown in Fig. 4; this experimental frame is described more fully by Lokkas (1996) and Lokkas and Croll (1998). It has elastic properties $EI_1 = 2.51 \times 10^4$ kN·mm^2, $EI_2 = EI_3 = 4.18 \times 10^4$ kN·mm^2, where I_i is the second moment of area for member i, and for the case of calculating critical loads the independent, nonproportionate loadings $F_n = F_s = 0$.

Of the infinite number of possible buckling modes, Fig. 5 summarizes those associated with the lowest four critical

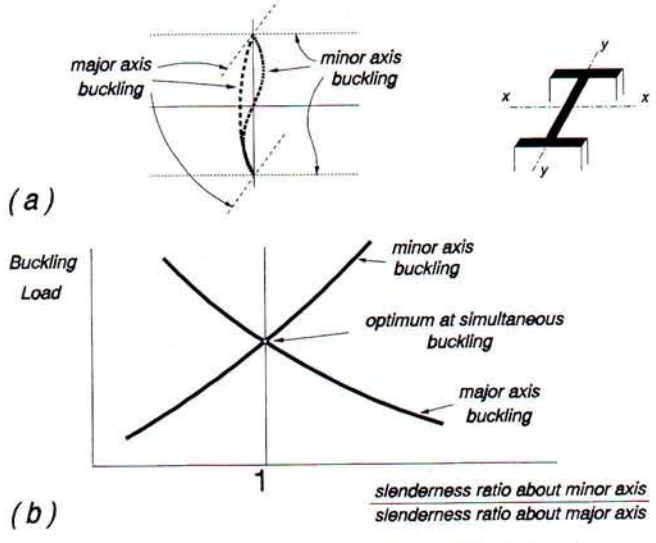

FIG. 2. Passive Interactive Buckling of Biaxial Column

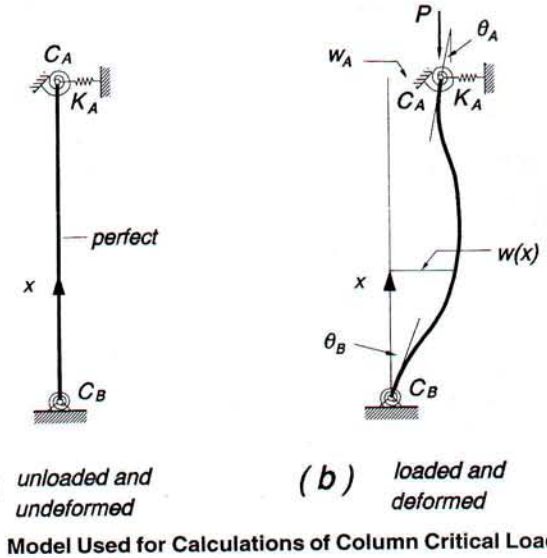

FIG. 3. Model Used for Calculations of Column Critical Loads

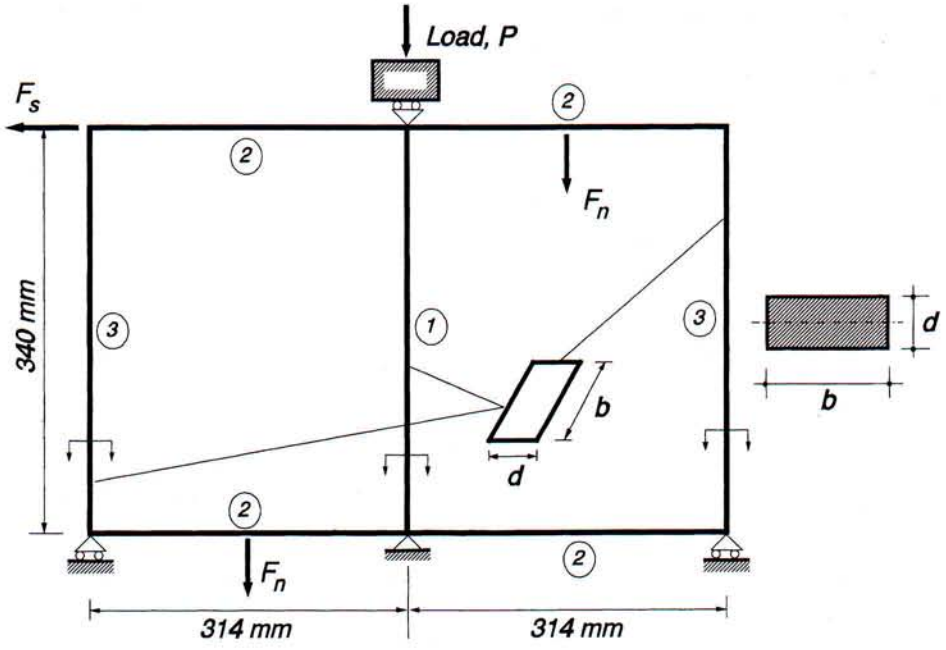

FIG. 4. Schematic Representation of Experimental Limited Frame

loads. This elastic critical load analysis has been undertaken using a specifically written finite-difference code described by Lokkas (1996). It is evident that while the lower two occur at similar load levels, the third and fourth modes are associated with considerably higher critical loads. This is apparent from the effective lengths. It might be observed that for the particular form of frame chosen, the single load at the central column is responsible for destabilizing all three columns in the sway mode. It is for this reason that despite its somewhat greater effective length, the sway mode has a higher critical load. Although this would be an unusual situation in real frames, the intention to develop and test experimental models covering a wide range of critical load ratios P_{cn}/P_{cs} governed the choice of the model frame of Fig. 4. This allows exploration of the situations that can occur in real frames where, as a combined result of the additional destabilization when all columns are loaded and the additional stabilization from other frame bracing against lateral deformation, it is possible for P_{cn}/P_{cs} to approach unity.

In subsequent analysis it will be useful to represent the critical mode shapes w_{ci} in normalized form

$$w_{ci}(x) = \bar{w}_{ci}\varphi_i(x) \tag{1}$$

The normalized mode shapes have been chosen so that the amplitudes $\bar{w}_{ci}$ represent the amplitudes over the effective lengths L_{ci}; these are indicated in Fig. 5. Although not the most convenient method of normalizing the mode shapes, it will be shown later to have the analytical advantages in defining the governing imperfection parameters and consequently the failure condition. These modal amplitudes can be thought of as representing the maximum displacement in the equivalent simply supported column having the appropriate effective length. It is a simple matter to relate these modal amplitudes to the physically more convenient amplitudes measured from the undeformed line of the column.

Elastic Nonlinearities

A typical column within a real frame will be subject to a number of effects other than just that of the axial load P. For example, the column will not be perfectly straight. This means that an axial load will from the outset induce bending. If the out-of-straightness $w^o(x)$ is represented in terms of the modal amplitudes $\bar{w}_i^o$, such that

$$w^o(x) = \sum_i \bar{w}_i^o\varphi_i(x) \tag{2}$$

where φ_i = normalized critical modes; then, provided deflection levels are kept to within practically acceptable limits, the total displacement w may be expressed as

$$w(x) = \sum_i \frac{P_{ci}}{(P_{ci} - P)}\bar{w}_i^o\varphi_i(x) \tag{3}$$

The change in displacement from the imperfect geometry, referred to as the incremental displacement v would be

$$v(x) = \sum_i \frac{P}{(P_{ci} - P)}\bar{w}_i^o\varphi_i(x) \tag{4}$$

which, if it is assumed that the geometrically imperfect column is stress-free, is the displacement that results in bending stresses. In a similar way, laterally applied loads and end moments and shears arising from the effects of loading in the frame, not proportional to axial load P will in the absence of axial load P induce a further displacement $w^N(x)$, which may also be represented as

$$w^N(x) = \sum_i \bar{w}_i^N\varphi_i(x) \tag{5}$$

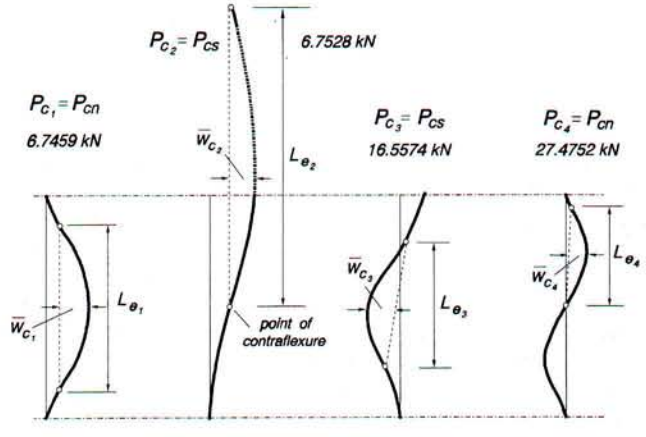

FIG. 5. Lowest Four Critical Loads and Mode Shapes in Central Column 1 of Limited Frame Example of Fig. 4

Unlike the geometric imperfection, the column will contain bending stresses associated with the nonproportionate loading imperfection $w^N(x)$. In other respects however the response will be similar, in that the total deformation is

$$w(x) = \sum_i \frac{P_{ci}}{(P_{ci} - P)} \bar{w}_i^N \varphi_i(x) \tag{6}$$

and the incremental displacement

$$v(x) = \sum_i \frac{P}{(P_{ci} - P)} \bar{w}_i^N \varphi_i(x) \tag{7}$$

Finally, there would be a third source of imperfection that arises from lateral loads and end moments that are proportional to P. If $e^P(x)$ represents the distribution of the transverse displacement caused by a unit load P, and

$$e^P(x) = \sum_i \bar{e}_i^P \varphi_i(x) \tag{8}$$

where $\bar{e}_i^P$ = modal amplitudes, then again, the total deformation (which in this case is also the incremental deformation) at load P will be

$$w(x) = \sum_i \frac{P_{ci}}{P_{ci} - P} P\bar{e}_i^P \varphi_i(x) \tag{9}$$

Combining (4), (7), and (9) and introducing the equivalent proportional load imperfection

$$\bar{w}_i^P = P_{ci}\bar{e}_i^P \tag{10}$$

the total incremental displacement may be written

$$v(x) = \sum_i \frac{P}{(P_{ci} - P)} \xi_i \varphi_i(x) \tag{11}$$

where the total equivalent modal imperfection is

$$\xi_i \equiv \bar{w}_i^o + \bar{w}_i^N + \bar{w}_i^P \tag{12}$$

and $\bar{w}_i^P$ has the meaning given in (10).

It is significant that all of the elastic nonlinearities can in each mode be encapsulated in terms of a single total equivalent modal imperfection. Although the modal representation of (11) is within the limitations of the so-called linearized modeling of columns, it is just those modes associated with the lowest critical loads that will in general be responsible for most of the resulting nonlinear elastic behavior. When added to the average stress caused by the axial load and the linear bending stress induced by all of the loads not proportional to the axial load P, it is the bending stresses associated with the nonlinear incremental displacement $v(x)$ that will be responsible for failure. With these incremental stresses directly dependent upon ξ_i, which in turn will generally have three independent contributions, it follows that any properly constituted failure criteria needs to make explicit reference to the total equivalent modal imperfections.

FAILURE CRITERIA

There are two conditions often used to define failure. As a lower bound, to collapse is the load at which first material yield occurs; this can for restrained columns lead to overly conservative estimates of elastic-plastic collapse. An alternative and usually somewhat better approximation of collapse is often provided by the load corresponding with first full section plasticity. For both of these criteria it is necessary to calculate the total moments in the column.

If the linear moments $m^N(x)$ associated with the nonproportionate imperfections $w^N(x)$, given by (5), are separated out from those caused by the incremental displacements, it is possible to write the total moment as

$$m(x) = m^N(x) + EIv''(x)$$

In this expression v'' represents the curvature of the summed incremental displacements from (11). Hence

$$m(x) = m^N(x) + EI \sum_i \frac{P}{(P_{ci} - P)} \xi_i \varphi_i''(x) \tag{13}$$

in which the total equivalent modal imperfection ξ_i is defined in (12).

First Yield

At any location along the column, the maximum axial stress will be given by

$$\sigma_m = \frac{P}{A} + \frac{m}{S} \tag{14}$$

where A = cross-sectional area; and S = elastic section modulus. On the basis of the total moments given by (13), and restricting the nonlinear effects to only the sway and lowest nonsway modes, with critical loads P_{cs} and P_{cn}, the maximum stress at any location over the column length may be represented as

$$\sigma_m = \frac{P}{A} + \frac{m^N}{S} + \frac{EI}{S}\left[\frac{P}{(P_{cs} - P)} \xi_s \varphi_s'' + \frac{P}{(P_{cn} - P)} \xi_n \varphi_n''\right]$$

Limiting the maximum stress at any location along the length of the column to the material yield σ_y writing

$$EI\varphi_s'' = \alpha P_{cs} \cdot \psi_s(x); \quad EI\varphi_n'' = \beta P_{cn} \cdot \psi_n(x) \tag{15a,b}$$

and introducing the squash load P_p representing the load to produce first yield in the presence of just the linear moments which is defined as

$$\frac{P_p}{P_y} = 1 - \left|\frac{m^N}{m_y}\right| \tag{16}$$

where $P_y = \sigma_y A$ and $m_y = \sigma_y S$, this first yield condition may be represented as

$$(P_p - P_1) = \frac{P_{cs}P_1}{(P_{cs} - P_1)} \cdot \frac{\xi_s A \alpha \psi_s}{S} + \frac{P_{cn}P_1}{(P_{cn} - P_1)} \cdot \frac{\xi_n A \beta \psi_n}{S} \tag{17}$$

in which $P_1 = P_{fy}$ represent the axial load corresponding with first yield. In these expressions, α and β are curvature parameters, and ψ_s and ψ_n are modified normalized modal curvature functions. Approximations for these will be provided later.

Introducing the notation that

$$p_1 \equiv P_1/P_p; \quad p_{cn} \equiv P_{cn}/P_p; \quad p_{cs} \equiv P_{cs}/P_p \tag{18a–c}$$

the nondimensionalized first yield condition may finally be written

$$p_1^3 + a_2 p_1^2 + a_1 p_1 + a_0 = 0 \tag{19}$$

In this expression

$$a_0 = -p_{cs}p_{cn}; \quad a_1 = +p_{cs}p_{cn}(\rho_s + \rho_n + 1) + p_{cs} + p_{cn}$$

$$a_2 = -(p_{cs}\rho_s + p_{cn}\rho_n + p_{cs} + p_{cn} + 1)$$

and the composite sway and nonsway imperfection parameters are

$$\rho_s \equiv \alpha\psi_s \cdot \frac{\xi_s A}{S}; \quad \rho_n \equiv \beta\psi_n \cdot \frac{\xi_n A}{S} \tag{20a,b}$$

The solution of (19) can be seen to depend upon only four parameters: the ratios of the two critical loads to the squash load and the two independent imperfection parameters.

It might be observed that when $\rho_s \to 0$, (16) factorizes into

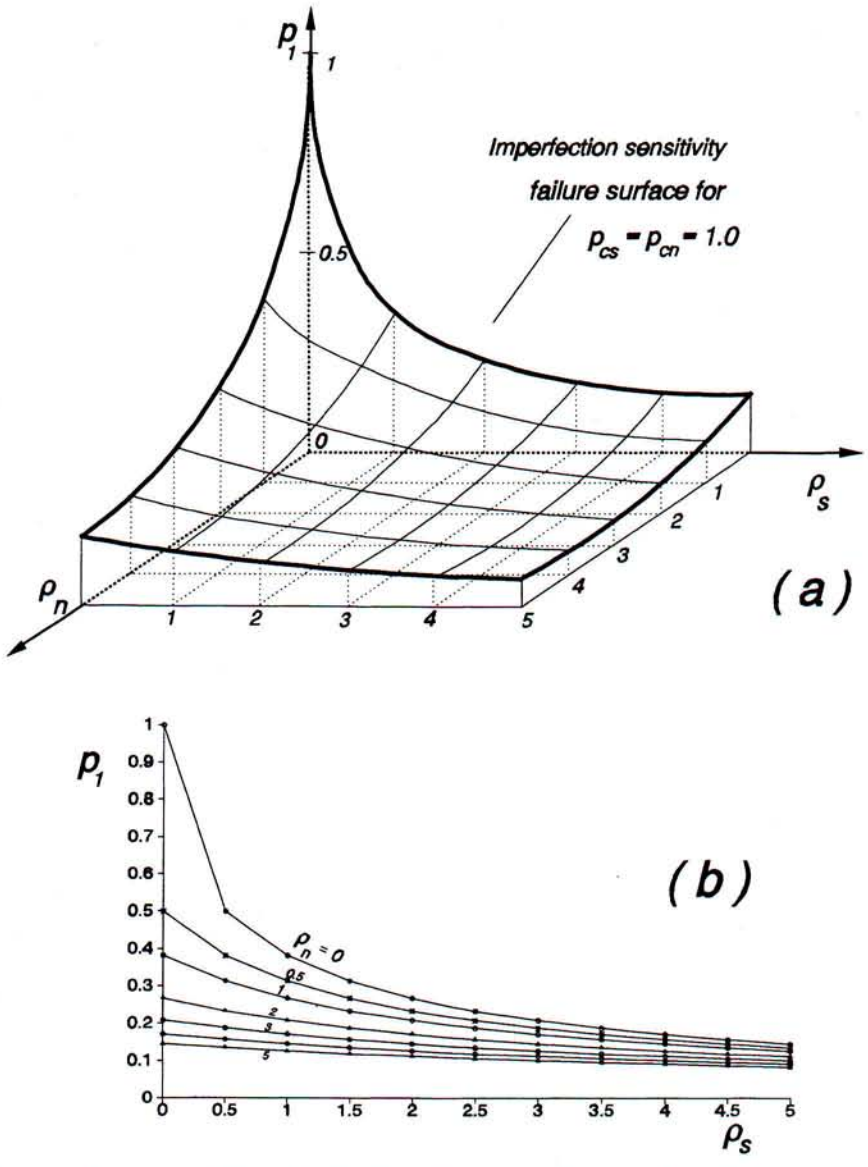

FIG. 6. Solutions to Eq. (19) Showing Imperfection Sensitivity Surface for First Yield

$$+(p_1 - p_{cs})[(p_1 - p_{cn})(p_1 - 1) - \rho_n p_1 p_{cn}] = 0 \qquad (21)$$

for which the expression in square brackets represents the well-known Ayrton-Perry criterion for single mode nonsway buckling. In an analogous way, (19) reduces to the Ayrton-Perry criterion for sway buckling when $\rho_n \to 0$.

To illustrate the nature of the imperfection sensitivity surface for first yield, Figs. 6(a and b) show the situation for $p_{cs} = p_{cn} = 1$. Just as in single mode buckling the sensitivity of buckling loads to imperfections is at its most extreme when the critical loads equal the squash load. Hence, for values of p_{cs} and p_{cn} not equal to unity the reductions in first yield p_1 with increasing ρ_s and ρ_n will be less extreme than those shown in Fig. 6. What Figs. 6(a and b) demonstrate is the potential importance of both modal imperfections in controlling the combined sway and nonsway buckling of frames. It is perhaps worth stressing that the imperfection sensitivities, shown for example in Figs. 6(a and b), would apply to any form of column cross section. In contrast, with most design practice, there is no need to produce different curves for various classes of column cross sections, because the cross section parameters are implicit in the definition of the imperfection parameters ρ_s and ρ_n of (20). Also, in contrast with most current design practice, the imperfection sensitivities, similar to those in Fig. 6, also contain the effects of interactions with frame moments as a result of the definition of the squash load P_p in (16). Furthermore, this compact presentation contains full allowance of the nonlinear effects arising from the imperfections associated with these frame moments, as required by the definition of the total equivalent modal imperfections ξ_i. Following the practice in most current design guidance would result in extremely cumbersome multiparameter presentations if the full effects of modal interactions are to be captured.

However, first yield often represents a fairly pessimistic lower bound to the actual buckling of frames. For this reason a second buckling failure criterion will be developed.

First Full Plasticity

For a rectangular cross section a fully plastic stress block corresponds to the plastic criterion

$$\frac{m}{m_p} = 1 - \left(\frac{P}{P_y}\right)^2$$

where $m_p = \sigma_y Z$, $P_y = \sigma_y A$, and $Z = bd^2/4$ = plastic section modulus. On the basis of the moment given by (13), and again taking only the first two critical modes, this plasticity criterion gives

$$\frac{m^N}{m_p} + \frac{EI}{m_p}\left[\frac{P}{P_{cs} - P}\xi_s\varphi_s''(x) + \frac{P}{P_{cn} - P}\xi_n\varphi_n''(x)\right] = 1 - \left(\frac{P}{P_y}\right)^2 \tag{22}$$

Introducing the modified squash load P_p^*, which represents the load to produce a fully plastic section in the presence of only the linear moments, defined as

$$\left(\frac{P_p^*}{P_y}\right)^2 = 1 - \left|\frac{m^N}{m_p}\right| \tag{23}$$

then (22) may be written

$$(P_p^{*2} - P_2^2) = \frac{AP_y}{Z}\left[\frac{P_2P_{cs}\xi_s\alpha\psi_s}{(P_{cs} - P_2)} + \frac{P_2P_{cn}\xi_n\beta\psi_n}{(P_{cn} - P_2)}\right] \tag{24}$$

where $P_2 = P_{fp}$ represents the axial load corresponding with a fully plastic section. Parameters α and β and the curvature distributions ψ_s and ψ_n have the same meaning as for the first yield condition of (17) and will be discussed further in the next section.

In analogy with the presentation of first yield, use of the nondimensional notation

$$p_2 \equiv P_2/P_p^*; \quad p_{cn} \equiv P_{cn}/P_p^* \tag{25a,b}$$

$$p_{cs} \equiv P_{cs}/P_p^*; \quad p_y \equiv P_y/P_p^* \tag{25c,d}$$

allows the full plasticity condition to be written

$$p_2^4 + b_3p_2^3 + b_2p_2^2 + b_1p_2 + b_0 = 0 \tag{26}$$

in which

$$b_0 = -p_{cs}p_{cn}; \quad b_1 = +(p_{cs} + p_{cn}) + p_{cs}p_{cn}(\rho_s^* + \rho_n^*)$$

$$b_2 = +p_{cs}p_{cn} - p_{cs}\rho_s^* - p_{cn}\rho_n^* - 1; \quad b_3 = -(p_{cs} + p_{cn})$$

and the composite sway and nonsway imperfection parameters are

$$\rho_s^* = p_y\alpha\psi_n\cdot\frac{A\xi_s}{S}; \quad \rho_n^* = p_y\beta\psi_s\cdot\frac{A\xi_n}{S} \tag{27a,b}$$

Solution of (26), to find the load giving full plasticity at a given location, can again be seen to depend upon four nondimensional parameters closely related to those of (19) for first yield: the ratios of the critical loads to the squash load p_{cs} and p_{cn} and the two imperfection parameters ρ_s^* and ρ_n^*. Imperfection parameters ρ_s^* and ρ_n^* can be determined from ρ_s and ρ_n of (20) by weighting with the cross section plasticity factor $p_y(S/Z)$ defined in (25).

Again, when $\rho_s^* \to 0$, (26) can be shown to factorize into the form

$$(p_2 - p_{cs})[(p_2^2 - 1)(p_2 - p_{cn}) - p_2p_{cn}\rho_n^*] = 0 \tag{28}$$

with one upper limit being given by $p_2 = p_{cs}$ and the other from the lowest of the solutions to the expression in square brackets. This single mode solution for full plasticity in the nonsway mode

$$(p_2^2 - 1)(p_2 - p_{cn}) - p_2p_{cn}\rho_n^* = 0 \tag{29}$$

has at times been referred to as the extended or "generalized" Ayrton-Perry buckling criterion. Equally, when $\rho_n^* \to 0$, (26) factorizes into an analogous form to (28) with an extended Ayrton-Perry buckling criterion for the sway mode taking the same form as (29).

A typical form of the imperfection sensitivity surface is shown in Fig. 7, for the case of $p_{cs} = p_{cn} = 1$; again, it is for coincidence of the sway and nonsway critical loads and the squash load that this surface exhibits its most extreme sensitivity to the imperfection parameters ρ_s^* and ρ_n^*. Provided the appropriate values of p_{cs}, p_{cn}, ρ_s^*, and ρ_n^* are used, solutions of (26) [similar to those shown in Figs. 7(a and b)] apply at any point over the column length. However, it is generally only important to check certain critical locations, as discussed in the next section.

Comparing Figs. 6 and 7 it can be seen that for given values of p_{cs} and p_{cn} and imperfection parameters ρ_s and ρ_n, the values of p_1 and p_2 are almost identical. This result can be shown to hold over the entire range of values of p_{cs}, p_{cn}, ρ_s, and ρ_n. It should be emphasized that this does not imply that the actual values of first yield load P_{fy} and full plasticity load P_{fp} are equal, as the squash load normalizations used for p_1 and p_2 are, respectively, P_p as given by (16) and P_p^* defined in (24). Furthermore, because the imperfection parameters ρ_s^* and ρ_n^* are related to those of ρ_s and ρ_n by the weighting factor $p_y(S/Z)$, where p_y is itself an implicit function of the linear nonproportional moment m^N, the values of p_1 and p_2 would not be equal for set values of the total equivalent imperfections ξ_s and ξ_n. However, the consideration that the solutions of (19) and (26) are so similar does have important consequences with regards to the presentation of design charts that rationally represent the effects of total imperfections. It means that a single series of charts could be used for the presentation of either P_{fy} or P_{fp}. It also means that the considerably simpler and somewhat conservative values of p_1 could be used to obtain estimates of p_2 and consequently P_{fp}.

Governing Imperfection Parameters

Eqs. (19) and (26) determine the loads required to produce first yield and full plasticity on any section over the length of the column, respectively. Not only do the imperfection parameters ρ_s, ρ_n, ρ_s^*, and ρ_n^* vary over the column length but so also do P_p and P_p^*. Clearly, in most practical circumstances there will be certain critical sections that govern the design of the column. For the experimental frame of Fig. 4 these critical sections will occur at column midlength, where the nonsway deformations produce their greatest curvature, and at the ends of the column, where the sway deformation has its greatest curvature. At midlength the sway deformation generally has very low curvature, and consequently there will be little modal interaction. At the ends, however, both the sway and the nonsway modes will produce significant buckling curvature represented by the imperfection parameters ρ_s and ρ_n for first yield and ρ_s^* and ρ_n^* for full plasticity. With the linear nonproportionate loading moments m^N also generally being at their greatest at the ends of the column, and hence P_p and P_p^* at their lowest values, it is upon these locations that attention will be focused.

As illustrated in Fig. 8(a), the nonsway mode may be represented as

$$w_{c_n}(x_1) = \bar{w}_{c_n}\sin\frac{\pi x_1}{L_{c_n}} \tag{30}$$

where on the basis of (15) $\varphi_n \equiv \sin(\pi x_1/L_{c_n})$. It follows from (15) that for the nonsway mode $|\psi_n| = \sin(\pi x_1/L_{c_n})$ and $\beta = 1$. Hence, at the ends of the column

$$|\psi_{n_c}| = \sin\frac{\pi(L - L_{c_n})}{2L_{c_n}} \tag{31}$$

and so for use in (19) and (26)

$$\rho_n = \sin\frac{\pi(L - L_{c_n})}{2L_{c_n}}\cdot\frac{A\xi_n}{S}; \quad \rho_n^* = p_y\cdot\sin\frac{\pi(L - L_{c_n})}{2L_{c_n}}\cdot\frac{A\xi_n}{Z} \tag{32a,b}$$

In an analogous way the sway mode on the basis of the coordinate system used in Fig. 8(b), may be written

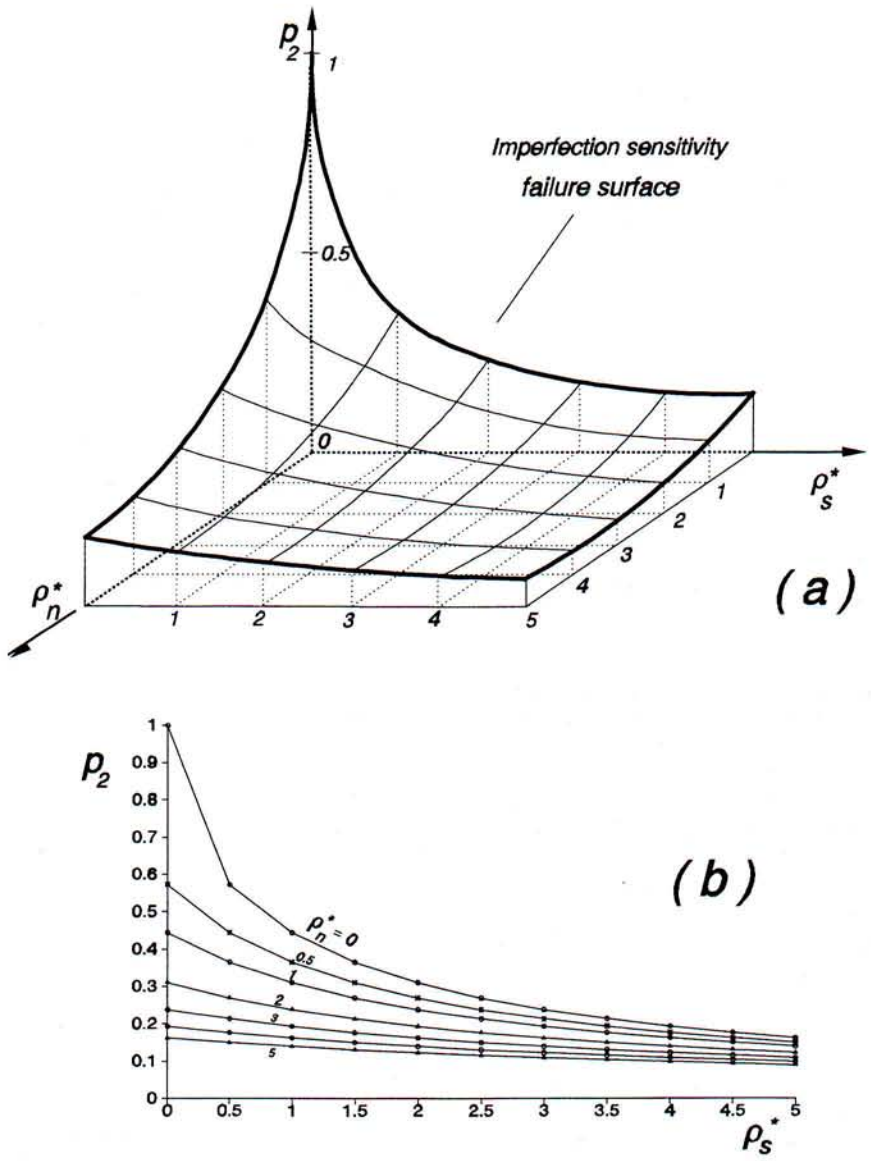

FIG. 7. Solutions to Eq. (26) Showing Imperfection Sensitivity Surface for Full Plasticity

$$w_{c_s}(x_2) = \bar{w}_{c_s} \sin \frac{\pi x_2}{L_{c_s}} \tag{33}$$

so that in (15) $\varphi_s = \sin(\pi x_2/L_{c_s})$. It follows that

$$\alpha = \frac{EI\left(\frac{\pi}{L_{c_s}}\right)^2}{P_{cs}} \tag{34}$$

and α represents the ratio of critical load of a simply supported column having effective length L_{c_s} to the actual sway critical load. This enhancement of P_{cs}, relative to that of a simply supported column of effective length L_{c_s}, is due to the additional stiffening coming from the lateral spring stiffness K_A. At the ends of the column

$$|\psi_{s_c}| = \sin \frac{\pi L}{2L_{c_s}} \tag{35}$$

In this case the governing sway imperfection parameters for (19) and (26) will be, respectively

$$\rho_s = \frac{\pi^2 EI}{L_{c_s}^2 P_{cs}} \cdot \sin \frac{\pi L}{2L_{c_s}} \cdot \frac{A\xi_s}{S}; \quad \rho_s^* = p_y \frac{\pi^2 EI}{L_{c_s}^2 P_{cs}} \cdot \sin \frac{\pi L}{2L_{c_s}} \cdot \frac{A\xi_s}{Z} \tag{36a,b}$$

It should be emphasized that L_{c_n} and L_{c_s} are the effective lengths of an equivalent simply supported column having the same mode shape as those associated with the nonsway and sway modes, respectively.

EXPERIMENTAL CONFIRMATION

Making use of a specially designed limited frame, an extensive test program was implemented so that the validity of the interactive buckling theory can be tested over a representative range of critical load ratio P_{cs}/P_{cn} and lowest elastic critical to plastic squash load ratio P_c/P_y. To provide conditions in which interactive buckling is likely to be significant, frame geometries were chosen to cover the range $0.6 < P_{cs}/P_{cn} < 1.5$. To ensure the strongest effects of both sway and nonsway imperfections on observed elastic-plastic buckling loads, it was desired to make P_c/P_y as close as practical to unity; as a consequence of load limitations on the rig, the ratios chosen were restricted to lie in the range of $0.25 < P_c/P_y < 0.50$, which means the test results did not capture the most extreme forms of interactive imperfection sensitivity.

The frame is schematically represented in Fig. 4, with greater details provided by Lokkas (1996) or more accessibly by Lokkas and Croll (1998). Essentially, the test frame allowed failed central column 1 to be removed and replaced without necessarily replacing the rest of the frame. This was achieved

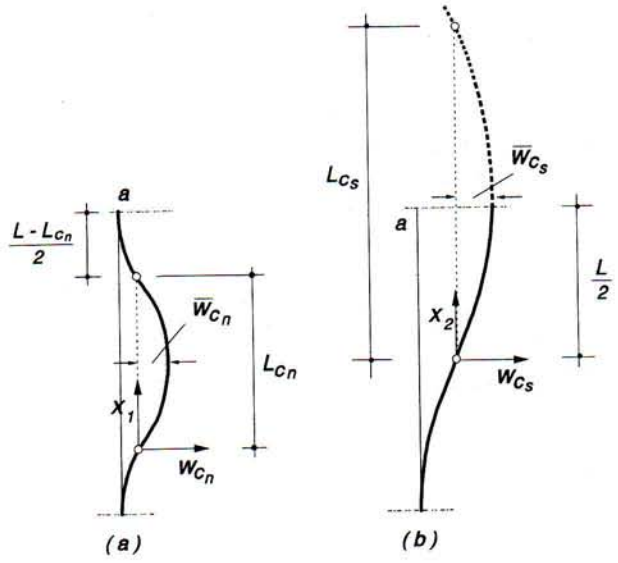

FIG. 8. Notation Used for Defining Curvature Parameters α, β, ψ_s, and ψ_n in Eq. (15)

by a series of mechanical clamps at each of the rigid joints, designed so that the column behavior was unimpeded over its entire length. By avoiding the more obvious use of welded joints, the uncertainties of the "heat affected zone" on plastic failure at the critical joint locations were overcome. However, these rigid clamps did result in other complications, not least being their effect upon the elastic rotational and translational stiffnesses restraining the ends of the columns. These effects were fully allowed for in the following theoretical calculations.

To enable controlled but independent variations in both the sway and nonsway total equivalent imperfections ξ_s and ξ_n, the loads F_n and F_s (Fig. 4) could be arbitrarily chosen. In a typical experiment, enough deformations were recorded over a sufficiently large number of increments in axial load to enable accurate Southwell plots to obtain best experimental estimates of both the sway and nonsway critical loads (P_{cs} and P_{cn}, respectively) and the associated total equivalent imperfections ξ_s and ξ_n. Together with the theoretical distributions of linear moment $m^N(x)$ over the column length, resulting from the application of loads F_n and F_s, these data then allowed calculations of the theoretical buckling estimates P_{fy} and P_{fp} from (19) and (26), which could then be compared with the actual experimental maximum, or buckling, loads P_b. In most cases the first yield and first hinge occurred as expected at the end of the column where the modal interactions are strongest. There were a few cases where the first plasticity was predicted to occur at the column midlength; in these cases the nonsway imperfection ξ_n dominated and the sway imperfection ξ_s was very small. The results are summarized in Fig. 9.

Experimentally inferred critical loads and modal imperfections were used in preference to the purely theoretical estimates. This was to overcome the uncertainties arising from the complexities of joint behavior. However, despite the inevitable uncertainties of joint rigidity, together with all the other sources of deviation between theory and experiment, it was shown by Lokkas and Croll (1998) that the experimentally determined critical loads were generally within $\pm 10\%$ of those predicted from theory.

It may be observed in Fig. 9(a) that first yield P_{fy} predictions from (19) represent, for the majority of tests, a reasonably close lower bound. The scatter generally lies within $\pm 20\%$, which might be expected in such a rigid jointed frame where total collapse generally requires the formation of more than one plastic hinge. As would be expected, the prediction of first full plasticity P_{fh} from (26) represents neither an upper nor a

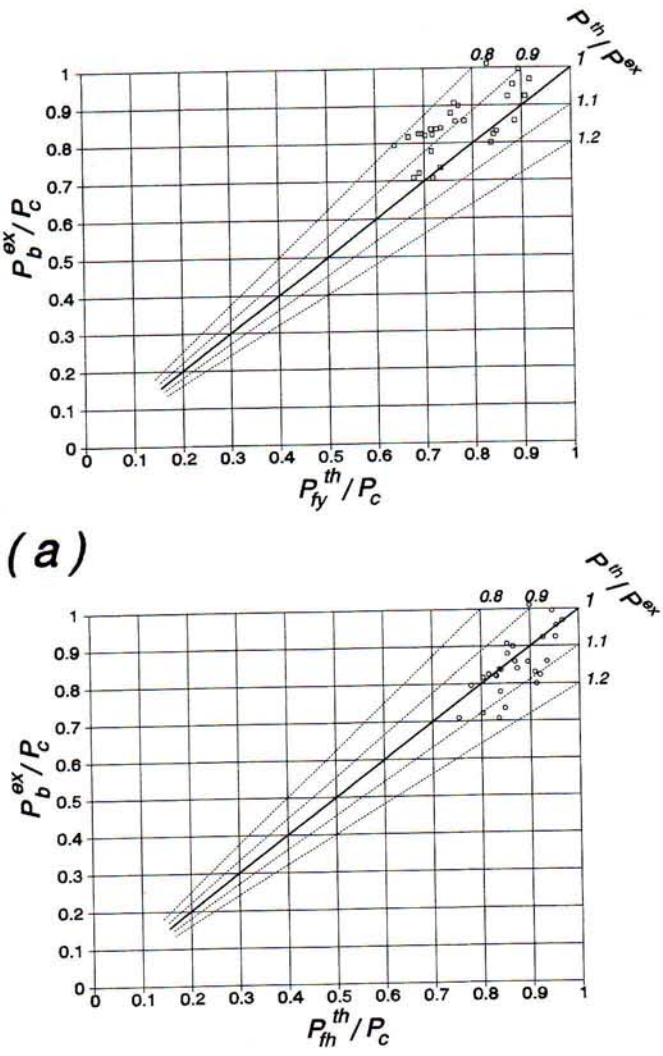

FIG. 9. Comparisons between Theoretical Calculations for Failure for: (a) First Yield; (b) Full Plasticity and Actual Experimental Buckling Loads

lower bound. Experimental buckling loads are generally scattered within the $\pm 10\%$ bands. To provide safe but reliable estimates of buckling collapse it would appear from these tests that the somewhat simpler first yield P_{fy} condition should be used. This is of course consistent with most existing design practice. Presentation of buckling collapse loads in Fig. 9 have been normalized with respect to the lowest critical load. This has the advantage of making clear what are the knockdowns due to imperfections. For the present tests the ratio of P_c/P_y did not exceed 0.5. It is for this reason that knockdowns due to interactive modal plasticity will be represented by the ratio p_b/p_c and are seen to be generally no lower than 0.7. Even so, these knockdowns are influenced significantly by both of the modal imperfections. If tests had been carried out on frames having $P_c/P_y \to 1$, the knockdowns produced by each of the interactive modes would be expected to be considerably higher.

CONCLUSIONS

It has been shown that, in circumstances where the sway and nonsway buckling loads for columns in framed structures are nearly equal, modal interactions can have an important influence upon buckling capacities. Two alternative theoretical estimates of buckling have been presented: (1) Material plasticity along the lines of the conventional Ayrton-Perry for-

mulas for single mode buckling; and (2) a first plastic hinge as a form of generalized Ayrton-Perry approach. In both theoretical methods the importance of providing adequate representations of the two modal imperfections has been emphasized, with the implicit suggestion that current design guidance even for single mode buckling, at times, leaves this too vague.

Comparisons with the results from a test program on model limited frames confirm the importance of modal interactions on buckling collapse behavior. These tests also provide reassurance as to the relevance of first plasticity theory, even for indeterminate rigid-jointed frames.

Although beyond the scope of the present paper, the systematic approach to the theoretical estimations of interactive column buckling loads, when simplified, is capable of straightforward incorporation into design practice. It is even possible that the approach described could greatly improve the treatment of single mode buckling adopted in current design practice.

APPENDIX I. REFERENCES

Gurfinkel, G., and Robinson, A. R. (1965). "Buckling of elastically restraint columns." *J. Struct. Div.*, ASCE, 91(6), 159–183.

Hopkins, H. J. (1990). *A span of bridges. An illustrated history*. Clarke Doble & Brendon Ltd., Plymouth, U.K.

Lokkas, P. (1996). "A consistent approach to the buckling design analysis of rigid jointed steel-frames subject to sidesway," PhD thesis, University College London, London.

Lokkas, P., and Croll, J. G. A. (1998). "Experimental investigation of combined sway and nonsway buckling of frames." *Proc., 11th Int. Conf. on Experimental Mech.*, Oxford, U.K.

"Specification for the use of structural steel in building." (1969). *BS 449*, British Standard Institution, London.

"Specification for unfired welded pressure vessels." (1976). *BS 5500*, British Standards Institute, London (amended April 1981).

"Steel structures, part 1.1." (1992). *Eurocode 3*, European Committee for Standardization, Brussels.

"Structural use of steelwork in building. Part 1." (1990). *BS 5950*, British Standard Institution, London.

APPENDIX II. NOTATION

The following symbols are used in this paper:

A = cross-sectional area;
C = rotational spring constant;
E = elastic modulus;
$e^P(x)$ = distribution of displacement caused by unit axial load;
I = moment of inertia;
K = translational spring constant;
L = length of column;
L_{c_n} = effective length of equivalent simply supported column having same mode shape as that associated with nonsway mode;
L_{c_s} = effective length of equivalent simply supported column having same mode shape as that associated with sway mode;
M = total bending moment;
M_y = yield moment ($=\sigma_y S$);
m_A, m_B = end-resistant moments;
m^N = linear bending moment associated with nonproportionate imperfections;
$m^N(x)$ = linear moments associated with nonproportionate imperfections;
m_p = plastic moment capacity ($=\sigma_y Z$);
P = axial load;
P_b = buckling load;
P_c = lowest elastic critical load;
P_{ci} = elastic critical load of ith critical mode;
P_{cn} = nonsway elastic critical load;
P_{cs} = sway elastic critical load;
P_E = Euler load;
P_p = squash load for first yield in presence of linear moments;
P_p^* = squash load for first full plasticity in presence of linear moments;
P_y = squash load in absence of bending moment ($=\sigma_y A$);
P_1 = first yield load ($=P_{fy}$);
P_2 = first full plasticity load ($=P_{fh}$);
p_{cs}, p_{cn} = first two nondimensional critical loads [$=(P_{cs}/P_p)$, (P_{cn}/P_p)], respectively;
p_1, p_2 = nondimensional load at first yield and full plasticity [$=(P_{fy}/P_p)$, (P_{fh}/P_p)], respectively;
$q^N(x)$ = transverse load in nonproportional loading system;
$w(x)$ = total deformation;
$\bar{w}_i^N$ = nonproportional (in absence of axial load) modal amplitude;
w^o = equivalent initial deflection (out-of-straightness);
$\bar{w}_i^o$ = out-of-straightness modal amplitude;
$\bar{w}_i^P$ = equivalent proportional load imperfection;
S, Z = elastic, plastic section modulus;
α = curvature parameter associated with sway critical mode;
β = curvature parameter associated with nonsway critical mode;
$v''(x)$ = curvature;
ξ_i = total equivalent modal imperfection;
ρ = imperfection parameter;
ρ_s, ρ_n = composite sway and nonsway dimensionless imperfection parameters corresponding with first yield;
ρ_s^*, ρ_n^* = composite sway and nonsway dimensionless imperfection parameters corresponding with fully plastic section;
σ = average compression stress ($=P/A$);
σ_y = yield stress;
ψ_n = modified normalized nonsway curvature function; and
ψ_s = modified normalized sway curvature function.

Subscripts

c = associated with elastic critical behavior;
i = associated with ith critical mode;
n = associated with elastic nonsway critical behavior; and
s = associated with elastic sway critical behavior.

Superscripts

N = associated with nonproportionate loading;
P = associated with proportionate loading.